[Article ID] 1003- 6326(2001)03- 0340- 05

Evolution of microstructure and dimension of as-molded parts during thermal removal process of wax-based MIM binder①

LI Yi-min(李益民), HUANG Bai-yun(黄伯云), LI Song-lin(李松林),
ZENG Zhou-shan(曾舟山), QU Xuan-hui(曲选辉)
(The National Key Laboratory for Powder Metallurgy,
Central South University, Changsha 410083, P. R. China)

[Abstract] The evolution of the microstructure and the dimension of as-molded parts were studied on the basis of the thermogravimetric analysis of wax-based MIM binder. The results show that the binder removal speeds are different in different temperature ranges during binder removal process. The evolution of the microstructure of as-molded parts during binder removal process clearly showed the initiation and formation of connected pore structure, which is the removal channel of the binder. The as-molded parts almost continuously shrank through binder removal process, except an expansion stage during 320~ 440 ℃, which is the dissolution expansion effect due to the dissolution of V_{PW} in the polymer melt.

[Key words] binder; as-molded parts; microstructure; dimension
[CLC number] TF 124.39 [Document code] A

1 INTRODUCTION

Metal Injection Molding (MIM) developed very fast as a kind of powder metallurgy net-shaping process in recent years. Introducing the idea of plastic injection molding, the binder is added into metal powders as the vehicle of flowability to get molded parts. The binder has to be removed before sintering to get full density or near full density parts[1~3]. The removal of the binder before sintering is very important because the binder occupies about 40% (volume fraction) in as-molded parts. The removal of the binder can be divided into two types: thermal removal and solvent extraction removal. Thermal removal is generally used in practice. There are some reports on the thermogravimetric analysis of the thermal removal of binder, the theoretic model of thermal removal, and the different laws of the removal of different binder components[4~12]. But there is no report on the observation of the evolution of the microstructure and the dimension of as-molded parts during thermal removal process to date. In present paper, the evolution of the microstructure and the dimension of as-molded parts during thermal removal process are studied on the basis of the thermogravimetric analysis for wax-based binder system.

2 EXPERIMENTAL

The metal powders used in the experiment were near spherical-sized carbonyl iron and nickel powder with the particle sizes of 4.0 μm and 2.6 μm respectively. The binder system was based on wax. The characteristics of binder components are shown in Table 1. PW, EVA, HDPE and SA in a mass ratio of 79∶10∶10∶1 were mixed on an impeller mixer to get the binder. The carbonyl iron and nickel powders were premixed on a V-type mixer in a mass ratio of 98∶2 for 8 h. The feedstock was prepared by mixing the binder with Fe-2Ni premixed powder in a powder loading of 58% (volume fraction) on a LH60 counter-rotating roller mixer. The TGA experiments were performed in nitrogen at a temperature ramp rate of 5 ℃/min on a Dupont 9900 thermal analyzer. The reference material was α-Al_2O_3. After granulating on a LSJ20 plastic extruder, the feedstock was injection molded on an SZ/28-250 injection molding machine to get as-molded disc-shaped parts, with a diameter of 20 mm and a thickness of 4 mm. The as-molded parts were thermally debound in nitrogen at a temperature ramp rate of 5 ℃/min on a tube furnace. Some compacts were taken out and weighed every 50 ℃ from 150 ℃ to 600 ℃. The microstructure of those compacts were investigated. Besides, some standard MIM tensile bars were prepared. The 15 mm gauge length was cut for thermal expansion test at a temperature ramp rate of 1 ℃/min on a DL-1500 dilatometer.

① [Foundation item] Projects (50044012 and 59634120) supported by the National Natural Science Foundation of China and project (99JY20048) supported by the Natural Science Foundation of Hunan Province [Received date] 2000- 05- 29; [Accepted date] 2000- 10- 21

Table 1 Characteristics of binder components

Component	Chemical composition	θ_m/ ℃	ρ/ (g·cm^{-3})
PW(paraffin wax)	C_nH_{2n+2}($20 \leqslant n \leqslant 40$)	58	0.91
HDPE(high density polyethylene)	$+CH_2-CH_2+_n$	139	0.98
EVA(polyethylene vinyl acetate)	$+(CHCOCH_3-CH_2)_x-(CH_2-CH_2)_y+_n$	80	0.96
SA(stearic acid)	$CH_3(CH_2)_{16}COOH$	66	0.96

3 RESULTS AND DISCUSSION

3.1 Mass loss curve at linear temperature ramp rate

The mass loss curve at a linear temperature ramp rate is shown in Fig. 1, in which curves 1 and 2 denote the mass loss of the pure binder and the as-molded parts respectively. It can be clearly seen that the removal rate of as-molded parts was much lower than that of the pure binder, and the linear temperature ramp resulted in different apparent appearances of compacts at different temperature stages. The different binder removal rates and different defects during each temperature range are shown in Table 2.

It can been seen from Fig. 1 and Table 1 that the TGA curve of the pure binder showed obvious regularity. About 80% binder was removed during 150~ 350 ℃ range. Because EVA just began to decompose, whereas HDPE had no decomposition at 350 ℃[6], PW was the only removed binder component. In other words, PW had been thoroughly removed at 350 ℃. The highest removal rate of PW was 8.26×10^{-5} g/(cm^2·s) during 250~ 300 ℃ range. The remained EVA and HDPE were removed during 350~ 550 ℃ range at a much lower rate compared to PW since EVA and HDPE had to be decomposed into small vapor molecular to be removed. For as-molded compacts, 22% binder was removed during 150~ 350 ℃ range, which means that there was still 60% PW remained in compacts. Two types of processes occur during the removal of the binder from compacts. One is the vaporization or thermal decomposition, which is a physical or chemical phase transformation process. Another is the transfer of the evaporated or decomposed binder components to the surface of compacts to escape into outer atmosphere, which is a physical heat and mass transfer process. For the binder system used in this paper, the thermal debinding can de divided into three stages[4]. The first is the initial pore structure formation stage, the second is the removal stage of remained PW after the formation of the connected pore structure, and the third is the last removal stage of remained EVA and HDPE. There was only about 20% binder removed during 150 ~ 350 ℃ range. Therefore it fell into the initial pore structure formation stage. The removal of the binder can be divided into the following steps during the initial pore structure formation stage: ① PW vaporizes to form V_{PW} and V_{PW} dissolves into EVA-HDPE polymer melt; ② V_{PW} diffuses to the interior surface, which

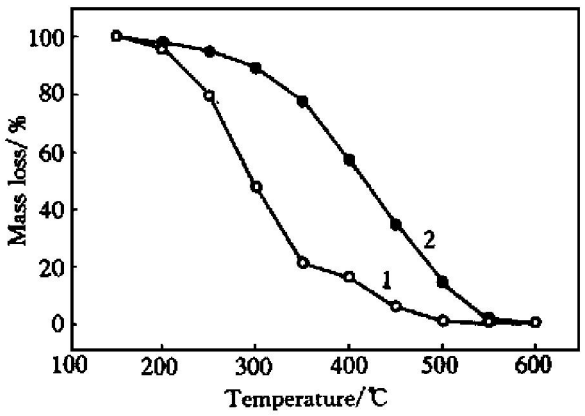

Fig. 1 Mass loss curve at linear temperature ramp rate

Table 2 Mass loss and apparent appearances of as-molded parts during different temperature ranges

Temperature range/ ℃	Binder removal rate for pure binder /(10^{-5} g·cm^{-2}·s)	Accumulative mass loss for pure binder/ %	Binder removal rate for as-molded parts /(10^{-5} g·cm^{-2}·s)	Accumulative mass loss for as-molded parts/ %	Apparent appearances of as-molded parts
150~ 200	1.08	4.2	0.52	2	Good
200~ 250	4.08	20	0.80	5.1	Good
250~ 300	8.26	52	1.47	11	Good
300~ 350	6.97	79	2.97	22	Good
350~ 400	1.29	84	5.33	43	Crack, deformation, blister
400~ 450	2.66	94	5.86	66	Crack, deformation, blister
450~ 500	1.29	99	5.27	84	Crack, deformation
500~ 550	0.18	100	3.15	98	Severe crack
550~ 600	0	100	0.46	100	Severe crack

is the binder-atmosphere interface, through the polymer melt; ③V_{PW} transfers to the surface of compacts through opened connected pore channel; ④V_{PW} escapes to the outer atmosphere. The control step is the liquid diffusion in step ②, i. e., the diffusion of V_{PW} in the polymer melts. The removal rate of the binder during 300 ~ 350 ℃ range was the highest from 150 ℃ to 350 ℃ and reached 2.97×10^{-5} g/(cm^2·s), which was the rate of liquid diffusion of V_{PW} in fact. The apparent appearance was still good up to now. That meant there still existed the equilibrium state and there was no macro defect produced, even there was about 60% PW evaporated to form V_{PW} and dissolved into the polymer melts, waiting for removal through the liquid diffusion.

EVA was partially discomposed into small vapor molecule to be removed during 350 ~ 400 ℃ range. The mass loss of EVA during this temperature range was small. But as-molded compacts showed large quantity of mass loss with high rate during this temperature range. The mass loss was 22% at the removal rate of 5.33×10^{-5} g/(cm^2·s). The accumulative mass loss reached 43%. It is suggested that the mass loss occurred during this temperature range mainly came from the remaining V_{PW} which was unable to be removed during former temperature range. The crack, deformation and blister defects appeared in as-molded compacts at this stage. Although the rate of liquid diffusion increased with the increase of temperature, the saturated vapor pressure of V_{PW} increased more rapidly at the same time. V_{PW} could not diffuse to the interior connected pore channel through the polymer melts. Therefore isolated bubbles were produced inside compacts. With the increase of the vapor pressure in isolated bubbles, some binder was pushed to the surface of compacts, leading to blister and deformation defects. On the other hand, crack defect occurred if the vapor pressure in bubbles exceeded the strength of compacts. The same processes occurred during 400 ~ 450 ℃ and 450 ~ 500 ℃ ranges.

When the temperature was increased to 500 ℃, 84% binder had been removed, which indicated that all PW had been removed, so as to a part of EVA and HDPE. The remained EVA and HDPE were removed during 500 ~ 600 ℃ range. There was no bubble found in compacts at this stage, but severe crack defect occurred, because all PW, which was the origin of bubbles, had been removed. There was only a little of liquid binder remained to bind powders and to keep the shape of compacts. The strength of compacts was very low at this stage. So the removal of the small vapor molecular, which was the decomposed product of EVA and HDPE, was very easy to cause severe crack defect since the internal stress exceeded the yield strength of compacts.

3.2 Evolution of microstructure of as-molded parts during removal of binder

The microstructures of as-molded parts, which were taken out every 50 ℃ beginning from 250 ℃, are shown in Figs. 2(a) ~ (i). The microstructure of as-molded parts at 250 ℃ is shown in Fig. 2(a). There was only a little of binder removed from the surface of compacts at this temperature. It can be seen that there were some empty pores formed between powder particles in compacts, but most of the pores were still filled with the binder. The initial removal process of the binder can be described as follows[4]. The formation rate of V_{PW} was the highest on the surface of compacts since the compact surface had the highest temperature at the beginning of thermal debinding process. Therefore V_{PW} was removed from the surface area of compacts firstly, which produced some small empty capillary pores in the surface area of compacts. Because of the difference of capillary force, these small empty capillary pores drew the binder from the comparatively bigger pores filled with the binder inside compacts to supplement the lost binder. Cima et al[13] observed the phenomenon in PVB-DBP binder system. Therefore, the content of EVA and HDPE in small surface capillary pores increased continuously with the removal of PW. On the other hand, V_{PW} had to diffuse to the binder/atmosphere interface through the EVA-HDPE melt to be removed. As V_{PW} was continuously produced and removed, small capillary empty pores, which took the similar function of the initial small surface capillary pores, occurred in areas inside compacts far from the compact surface. Now, the binder/atmosphere interface moved into the inside of compacts. V_{PW} only needed to diffuse to the interior surface of the capillary pores to escape to the atmosphere. So the formation of empty pores advanced towards the inside of compacts along the route of comparatively bigger pores. The connected pore structure began to be formed. The initial pore structure formation stage, in which there were a few small capillary pores occurred in the middle area of compacts, is shown in Fig. 2(b). The binder had capillary flow and redistribution at this stage. The SEM photograph at 350 ℃ is shown in Fig. 2(c). The microstructure was similar to that observed in Fig. 2(b), except that the quantity and volume of empty pores increased. The SEM photograph at 400 ℃ is shown in Fig. 2(d). It can be seen that the connected pore channel formed because 43% binder had been removed. The microstructure at 450 ℃ is shown in Fig. 2(e) with 66% binder removed. It can be found that there was binder-stringing phenomenon between powder particles, which came from the stringing effects of EVA and HDPE

because that most PW had been removed and the binding of powder particles only depended on EVA and HDPE. The microstructure at 500 ℃ is shown in Fig. 2(f). It can be found that the boundary of powder particles became clear. There was still some binder-stringing phenomenon between powder particles. The microstructure at 550 ℃ is shown in Fig. 2(g). It can be seen that the boundary of powder particles was very clear. The binder was almost completely removed now. The integrity of compacts depended on the friction between powder particles and very slight presintering effects. The microstructure shown in Fig. 2(h) represents the presintering state of powder particles. The microstructure of compacts after 700 ℃ presintering of 30 min is shown in Fig. 2(i).

3.3 Evolution of dimension of as-molded parts during removal of binder

The dilatometric curve of as-molded parts with the temperature ramp rate of 1 ℃/min is shown in Fig. 3. It can be seen that there was 0.4% expansion from 10 ℃ to 58 ℃, followed with continuous shrinkage. The melting point of PW was 58 ℃. The as-molded parts were in solid state below 58 ℃. Therefore, the observed expansion was supposed to be the thermal expansion. The expansion coefficient of solid PW was about 0.005 108[14], which was far higher than the observed expansion. The reason was that the powder framework in as-molded parts had little expansion. The as-molded parts shrank continuously from 58 ℃ to 320 ℃. The shrinkage reached

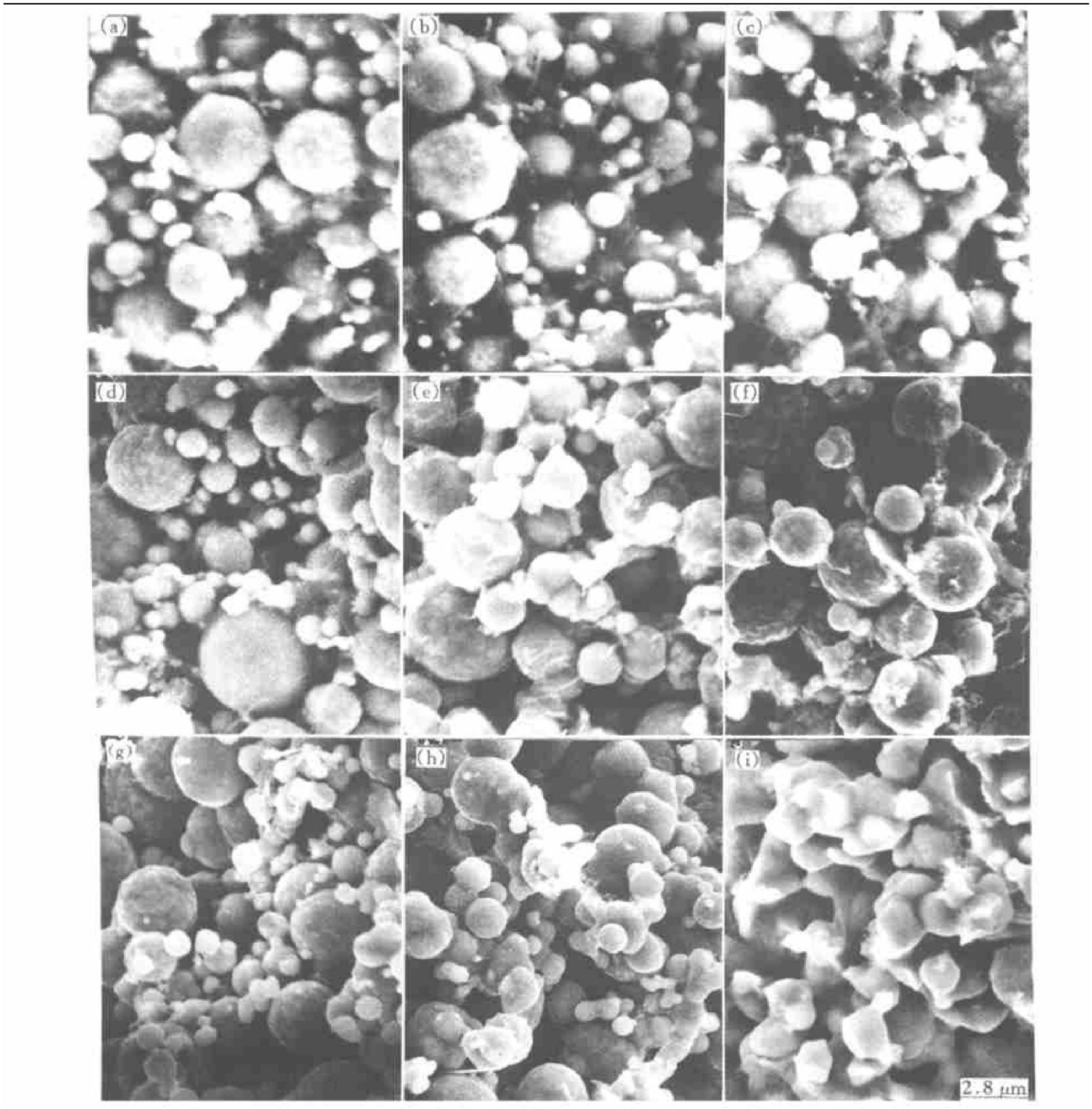

Fig. 2 Microstructure of as-molded parts during thermal removal of binder

3.7%. Referring to the data in Table 2, it can be seen that 22.3% binder was removed at 350 ℃ and 42.9% binder was removed at 400 ℃ under the temperature ramp rate of 5 ℃/min. Because the temperature ramp rate was 1 ℃/min in the dilatometry experiment, it was estimated that about 25% binder was removed at 320 ℃. With the binder continuously removed, as-molded parts shrank continuously.

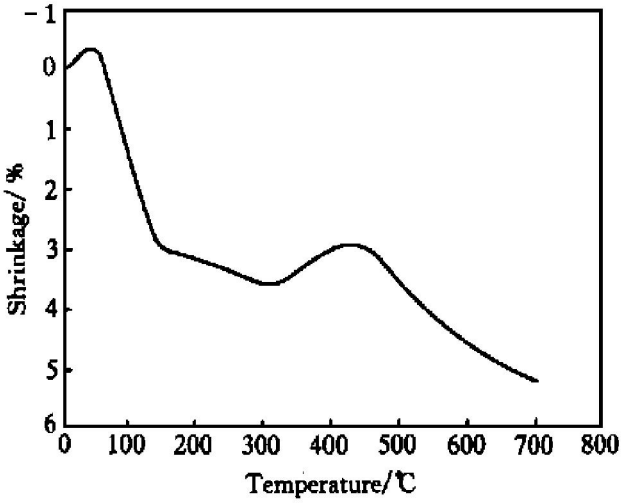

Fig. 3 Dilatometric curve of as-molded parts

The as-molded parts had the shrinkage of -1.2%, i.e. 1.2% expansion from 320 ℃ to 440 ℃. The shrinkage was 2.5% compared with the original parts. Although there was only 25% binder removed at 320 ℃, but PW had been evaporated completely to form V_{PW} referring to Fig. 1. V_{PW} dissolved into the polymer melts, waiting to be removed by diffusing to the interior surface of connected pore channel through polymer melts. Because the volume of V_{PW} was larger than that of L_{PW}, the dissolution of V_{PW} into the polymer melts led to the dissolution-expansion effect, so as-molded parts began to expand from 320 ℃. When the temperature was increased to 440 ℃, 70% binder was removed referring to Table 2. Since PW was almost completely removed, the dissolution-expansion released. As-molded parts no longer expanded and continued to shrink. The shrinkage was 5.2% after presintering at 700 ℃.

4 CONCLUSIONS

1) The binder removal speeds are different for different temperature ranges during binder removal process due to the difference of removal temperature ranges and removal laws for different binder components. If there were no corresponding temperature ramps for different temperature ranges, various defects would occur and destroy the integrity of as-molded parts.

2) The evolution of the microstructure of as-molded parts during binder removal process clearly shows the initiation and formation of connected pore structure, and the removal of the binder through connected pore channel.

3) After some thermal expansion during the initial solid state, the as-molded parts almost continuously shrank through binder removal process, except an expansion stage of 320~ 440 ℃, which is the dissolution expansion effect due to the dissolution of V_{PW} in the polymer melts.

[REFERENCES]

[1] LI Yi-min, HUANG Bai-yun, QU Xuan-hui. Today's metal injection molding technique [J]. Powder Metall Indus, (in Chinese), 2000, 10(1): 14- 19.

[2] German R M, Hens K F. Key issues in powder injection molding [J]. Ceram Bull, 1991, 70(8): 1294- 1302.

[3] German R M. Technological barriers and opportunities in powder injection molding [J]. Powder Metall Int, 1993, 25(4): 165- 169.

[4] LI Yi-min, QU Xuan-hui, HUANG Bai-yun. Thermal debinding and model of multi-polymer components wax-based MIM binder [J]. Acta Metall Sinica, (in Chinese), 1999, 35(2): 167- 171.

[5] LI Yi-min, HUANG Bai-yun, QU Xuan-hui. Rheological and debinding properties of thermoplastic wax-based MIM binder [J]. Chinese J Mater Res, (in Chinese), 1999, 13(6): 596- 600.

[6] LI Yi-min, HUANG Bai-yun, QU Xuan-hui. Step-by-step rapid debinding process of multi-polymer components wax-based MIM binder [J]. Rare Metal Mater Eng, (in Chinese), 2000, 29(1): 46-49.

[7] Angermann H H, Yang F K, Biest O V D. Removal of low molecular weight components during thermal debinding of powder-compacts [J]. J Mater Sci, 1992, 27: 2534- 2538.

[8] Calvert P, Cima M. Theoretical models for binder burnout [J]. J Am Ceram Soc, 1990, 73(3): 575- 579.

[9] Barone M R, Ulincy J C. Liquid-phase transport during removal of organic binders in injection-molded ceramics [J]. J Am Ceram Soc, 1990, 73(11): 3323- 3333.

[10] Hwang K S, Hsieh Y M. Comparative study of pore structure evolution during solvent and thermal debinding of powder injection molded parts [J]. Metall Mater Trans, 1996, 27A: 245- 253.

[11] LI Yi-min, HUANG Bai-yun, QU Xuan-hui. Improvement of rheological and shape retention properties of wax-based MIM binder by multi-polymer components [J]. Trans Nonferrous Met Soc China, 1999, 9(1): 22 - 29.

[12] Shaw H M, Edirsinghe M J. Binder degradation and redistribution during pyrolysis of ceramic injection mouldings [J]. J Mater Sci Letters, 1999, 12: 1227- 1230.

[13] Cima M J, Dudiziak M, Lewis J A. Observation of polyvinyl bulyral-dibutyl phthalate binder capillary migration [J]. J Am Ceram Soc, 1989, 72(6): 1087- 1090.

[14] Bennett H. Industrial Waxes [M]. New York: Chemical Publishing Company, Inc, 1975. 50.

(Edited by PENG Chao-qun)